



## Optical arbitrary waveform characterization using linear spectrograms

Zhi Jiang <sup>a</sup>, Daniel E. Leaird <sup>b</sup>, Christopher M. Long <sup>b</sup>, Stephen A. Boppart <sup>a</sup>, Andrew M. Weiner <sup>b,\*</sup>

<sup>a</sup> Beckman Institute for Advanced Science and Technology, University of Illinois at Urbana-Champaign, Urbana, IL 61801, United States

<sup>b</sup> School of Electrical and Computer Engineering, Purdue University, West Lafayette, IN 47907, United States

### ARTICLE INFO

#### Article history:

Received 23 November 2009

Received in revised form 27 March 2010

Accepted 30 March 2010

### ABSTRACT

We demonstrate the first application of linear spectrogram methods based on electro-optic phase modulation to characterize optical arbitrary waveforms generated under spectral line-by-line control. This approach offers both superior sensitivity and self-referencing capability for retrieval of periodic high repetition rate optical arbitrary waveforms.

© 2010 Elsevier B.V. All rights reserved.

### 1. Introduction

Pulse shaping techniques, in which intensity and phase manipulation of optical spectral components allow synthesis of user-specified ultrashort pulse fields according to a Fourier transform relationship, have been developed and widely adopted [1]. With the possibility to extend pulse shaping to independently manipulate the intensity and phase of individual spectral lines (line-by-line pulse shaping) [2], generation of periodic optical waveforms with essentially arbitrary features within each waveform period can be achieved. Optical Arbitrary Waveform Generation (O-AWG) resulting from line-by-line pulse shaping strives to combine the waveform control capabilities of pulse shaping with the long term coherence properties of frequency combs [3]. Spectral line-by-line pulse shaping and O-AWG have received considerable recent research attention [2,4–7] and have potential for broad impact in optical science and technology.

O-AWG leads to new challenges in ultrafast waveform characterization, since waveforms generated through line-by-line shaping exhibit several unique attributes. Such waveforms may exhibit 100% duty cycle, with shaped waveforms spanning the full time domain repetition period of the frequency comb, and with spectral amplitude and phase changing abruptly from line to line. Various methods for ultrashort pulse characterization, including frequency-resolved optical gating (FROG) [8], spectral shearing interferometry (SPIDER) [9], and tomography-based methods [10], are now well known. However, such methods are typically applied to measurement of low duty cycle pulses that are isolated in time, with spectra that are smoothly varying, and with relatively low time-bandwidth product. For high duty cycle periodic waveforms, including O-AWG waveforms based on spectral line-by-line pulse shaping, abrupt intensity/phase changes

from line to line pose new measurement challenges. In recent years several approaches to adapt existing methods to high spectral resolution operation required for O-AWG characterization have been reported [5,11–14].

Another measurement approach, based on linear spectrogram methods, is described in Refs. [15–20]. Linear spectrogram methods offer superior sensitivity, remarkable simplicity, and the capability to measure/resolve intensity/phase changes between individual spectral lines. Such techniques have been used for characterization of high rate telecommunications pulse trains, frequency combs generated by strong periodic phase modulation, as well as pulses distorted via linear and nonlinear propagation in fibers. However, these techniques have not been previously applied for characterization of optical arbitrary waveforms generated through line-by-line pulse shaping. Here, for the first time to our knowledge, we exploit the linear spectrogram method for characterization of O-AWG waveforms and demonstrate that this approach successfully is able to retrieve very rapid spectral phase changes inherent to line-by-line shaping. We show that spectral phase data retrieved using linear spectrograms to characterize frequency combs generated via strong periodic modulation is of sufficient quality to allow pulse shaper assisted compression to the bandwidth limit. We further show that such compressed pulses can be precisely reshaped into optical arbitrary waveforms via line-by-line shaping and then again precisely characterized using linear spectrograms.

Compared with other methods for O-AWG characterization, major advantages of the present linear spectrogram approach include the following: (1) it is a self-referenced technique, and therefore does not require a reference pulse as in Refs. [5,13]. In experiments such as ours based on a periodically modulated CW source [21,22], an independent reference pulse is generally not available. (2) The spectrogram technique is linear and does not require nonlinear optics and components compatible with the second harmonic wavelength as in Refs. [4,5,11,14]. High sensitivity is realized since no nonlinear optics is involved. (3) In contrast with non-iterative methods, e.g., [12], the

\* Corresponding author.

E-mail address: [amw@ecn.purdue.edu](mailto:amw@ecn.purdue.edu) (A.M. Weiner).

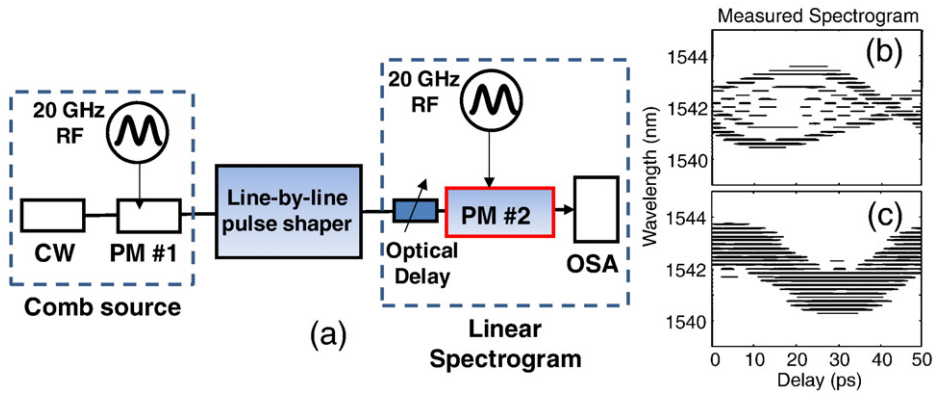


**Fig. 1.** (a) Experimental setup. PM: phase modulator. OSA: Optical spectrum analyzer. (b,c) Measured spectrogram corresponding to Figs. 2 and 3.

redundancy in the measured spectrogram and the iterative retrieval procedure ensure high measurement accuracy, similar to FROG [8]. Although linear spectrograms cannot be measured in a single shot, as is potentially possible with spectral interferometry methods [23–25], real time implementation of linear spectrogram waveform retrieval has been demonstrated at 10 Hz in Ref. [16]. A linear spectrogram method using an electro-absorption modulator has been used for feedback control of pulse shaping [26], but not in the line-by-line shaping regime demonstrated here.

In our particular implementation, we use a linear spectrogram method based on electro-optic phase modulation. Among various implementations of linear spectrograms, those using a phase modulator gate [18,19] provide broader measurement bandwidth [17] for characterization of shorter pulses and higher complexity broadband O-AWG signals. In addition to linear spectrogram methods using a phase modulator gate, nonlinear optical phase gates have also been used in both FROG and FROG-like measurements, both in the visible and near-infrared, e.g., [27,28], and as CRAB-FROG in attosecond science [29].

## 2. Results and discussion

**Fig. 1(a)** shows our experimental setup. For the signal field we start with a continuous-wave (CW) laser at 1542 nm, which is strongly phase modulated to produce a comb. Phase modulator #1, which is driven at an RF frequency equal to 19.906 GHz, leads to a comb consisting of approximately 13 discrete lines spaced by the repetition rate  $f_{\text{rep}} = 19.906$  GHz. At this point the signal is spread in time over the full comb repetition period. The phase-modulated CW laser is

followed by a line-by-line pulse shaper [2], which is used for O-AWG. A programmable optical delay, a second phase modulator, and an optical spectrum analyzer are used for O-AWG characterization using the linear spectrogram method. The RF driving signals for both phase modulators are synchronized.

Detailed discussion of linear spectrogram methods may be found in Refs. [15–18]. Briefly, the pulse or O-AWG field under test, designated  $a(t - \tau)$  after experiencing delay  $\tau$ , is multiplied by the phase modulator gate signal  $g(t)$ , and the optical power spectrum is measured for each delay  $\tau$ . Once the spectrogram is acquired by stepping the delay over one waveform period, a FROG-like algorithm [8,30] can be used to retrieve intensity/phase for both  $a(t)$  and  $g(t)$ .

**Fig. 1(b,c)** shows the measured spectrograms corresponding to Figs. 2 and 3, respectively. The spectrograms show discrete 20 GHz features of spectral line spacing as expected. The measured spectrogram is sampled to a  $64 \times 64$  grid by picking the spectral peak intensities of the spectral lines. Then, the vector-based principal component generalized projection algorithm described in Ref. [30] is used for both pulse  $a(t)$  and gate  $g(t)$  retrieval without any constraint as blind-FROG.

**Fig. 2** shows the retrieved pulse  $a(t)$ , gate  $g(t)$ , and corresponding spectra when the pulse shaper is quiescent (no spectral phase variation is applied). Although zero spectral phase is applied to the pulse shaper, the pulse shaper is not dispersion free and there is dispersion from fiber links as well. The phase modulation used to create  $a(t)$  combined with this dispersion results in a pulse-like feature on top of a large pedestal, as shown in **Fig. 2(a)**. Accordingly, the retrieved temporal phase of  $a(t)$  is a distorted sine waveform also evident in **Fig. 2(a)**. The spectral phase of  $a(t)$ , plotted in **Fig. 2(b)**, indeed shows quadratic phase structure on top of the irregular spectral phases caused by phase modulator #1. We will

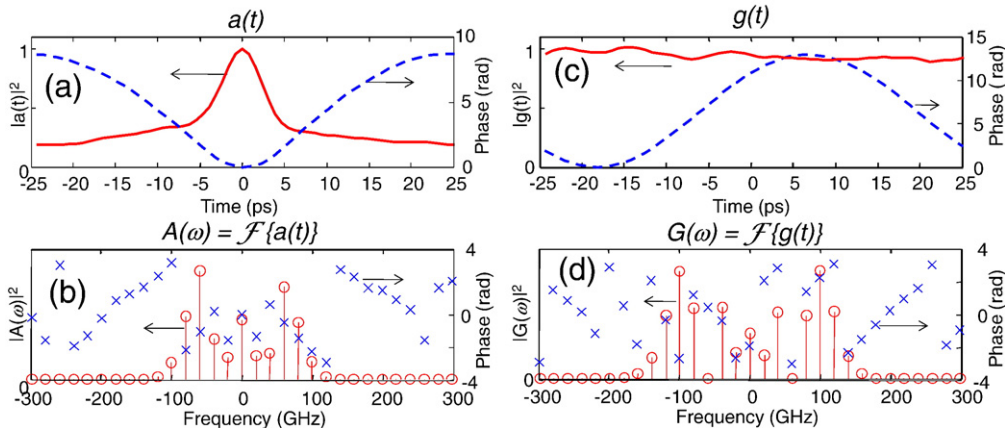


**Fig. 2.** Unshaped input. Intensity and phase of retrieved (a) pulse  $a(t)$ , (b) spectrum  $A(\omega)$ , (c) gate  $g(t)$ , and (d) spectrum  $G(\omega)$ . In (a) and (c), solid line: intensity, dashed line: phase. In (b) and (d), circles: intensity, crosses: phase.

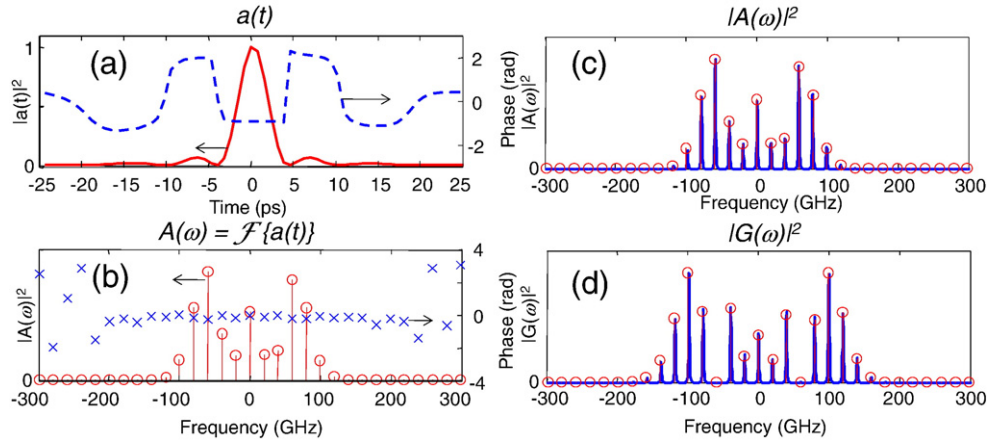


**Fig. 3.** Spectral phase of the input is compensated to obtain transform-limited pulse. (a) Pulse  $a(t)$ , (b) spectrum  $A(\omega)$ , (c) intensity of  $A(\omega)$ , and (d) intensity of  $G(\omega)$ . In (c) and (d), circles: retrieved, solid line: directly measured.

compensate the spectral phases using the line-by-line pulse shaper to achieve transform-limited pulses in the following experiments. The retrieved  $g(t)$  is phase-only modulated as shown in Fig. 2(c). Since we do not apply any constraint in our algorithm, the intensity of  $g(t)$  shows small ripples. We also tried constrained retrieval (not shown) by forcing the intensity of  $g(t)$  to be constant as in Ref. [18] and the results show that intensity and phase of  $a(t)$  as well as phase of  $g(t)$  are essentially unchanged. Actually the relatively small ripples as in Fig. 2(c) show that this method works well. The retrieved temporal phase of  $g(t)$  reflects the sinusoidal drive waveform applied to phase modulator #2, as expected. The retrieval error, similar to that defined in FROG algorithm, is typically below  $5 \times 10^{-3}$ .

In the next experiment, we used the line-by-line pulse shaper to apply the conjugate of the measured spectral phases of Fig. 2(b) to the input field  $a(t)$  to achieve transform-limited pulses. The retrieved spectral phases are essentially flat, as shown in Fig. 3(b), which demonstrates high precision of both O-AWG generation and O-AWG measurement using linear spectrograms. The temporal pulse in Fig. 3(a) has a pulse width of 3.8 ps (FWHM). The sidelobes of the temporal pulse have alternating phase shifts of  $\sim\pi$ . The retrieved gate  $g(t)$  (not shown) is essentially the same as in Fig. 2. Fig. 3(c) shows a comparison of the retrieved spectrum of pulse  $A(\omega)$  (circles) and its spectrum independently measured using an optical spectrum analyzer (solid line). The agreement is nearly perfect. Fig. 3(d) shows

similar comparison and agreement for the spectrum of gate  $G(\omega)$ . To measure the spectrum of the gate, we used a CW laser as input to phase modulator #2 and measured the output spectrum. We also performed independent intensity auto-correlation measurements using second harmonic generation and compared with the calculated intensity auto-correlation based on the retrieved pulse intensity in Fig. 3(a). The results (not shown) are essentially indistinguishable.

With the compensated transform-limited pulses as obtained in Fig. 3, we applied additional cubic spectral phase to explore examples of O-AWG. Fig. 4(a,b) shows the retrieved temporal and spectral profiles when a certain cubic spectral phase, designated  $\Phi(\omega)$ , is applied. The retrieved spectral phase (crosses) agrees closely with the spectral phase applied by the line-by-line pulse shaper (squares). Again this demonstrates high precision both in O-AWG measurement using linear spectrograms and O-AWG generation using spectral line-by-line pulse shaping. The temporal intensity shows a clear oscillatory tail – a well known property of cubic spectral phase. Fig. 4(c,d) shows the results when  $-\Phi(\omega)$  is applied, in which as expected the oscillatory tail now precedes the main pulse. Fig. 4(e,f) shows the results when  $-2\Phi(\omega)$  is applied. In all cases the retrieved spectral phases agree well with the cubic spectral phases applied by the line-by-line pulse shaper. With the larger cubic spectral phase, as shown in Fig. 4(e), the oscillatory tail becomes larger and spans the full waveform period – a key signature of line-by-line pulse shaping [2,4].

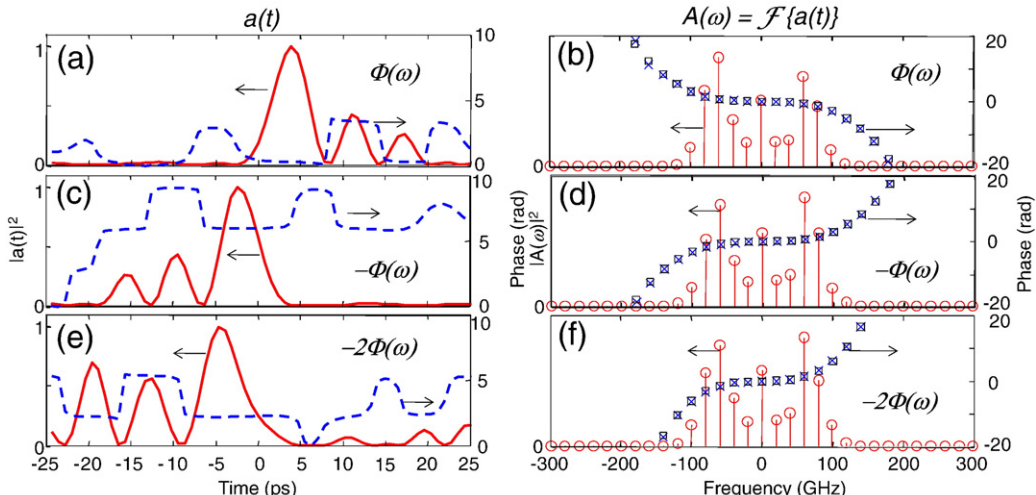


**Fig. 4.** Intensity and phase of retrieved pulse  $a(t)$  and spectrum  $A(\omega)$  with cubic spectral phases. (a,b): cubic spectral phase  $\Phi(\omega)$ . (c,d):  $-\Phi(\omega)$ . (e,f):  $-2\Phi(\omega)$ .

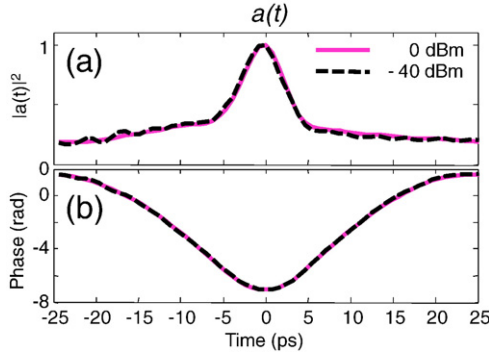


**Fig. 5.** Retrieved pulse  $a(t)$  with unshaped input. (a) Temporal intensity, (b) temporal phase. Solid line: 0 dBm, dashed line:  $-40$  dBm.

This example clearly demonstrates the ability of linear spectrogram methods to measure 100% duty cycle O-AWG waveforms with complexity sufficient to span to full temporal periodicity.

Finally, we demonstrate the superior sensitivity of the linear spectrogram method for O-AWG characterization. We program the pulse shaper for zero spectral phase and measure waveforms at both 0 dBm and  $-40$  dBm. A higher sensitivity setting of the OSA has been used for the  $-40$  dBm case which leads to longer data acquisition time. They agree with each other very well as shown in Fig. 5. The  $-40$  dBm power (100 nW) corresponds to a pulse energy of  $5 \times 10^{-18}$  Joule (5 aJ) at 20 GHz. This level of sensitivity is similar to previous reports using the linear spectrogram method [15].

Compared with an intensity modulator gate [15], the use of a phase modulator gate [18] is reported to provide much larger bandwidth to support measurement of shorter pulses and, more importantly here, O-AWG signals with broader bandwidth. This becomes increasingly important for characterization of high complexity O-AWG signals generated through spectral line-by-line pulse shaping, since waveform complexity is determined by the number of spectral lines, which is proportional to bandwidth [4]. In our experiments, the gate has a bandwidth of  $\sim 300$  GHz, which based on our simulations may be capable of measuring O-AWG signals with a bandwidth of  $\sim 2000$  GHz. This corresponds to  $\sim 200$  lines with 10 GHz line spacing.

To illustrate the practicality and robustness of extending this method to the 200 line regime, Fig. 6 shows simulated examples for a noise-free spectrogram and for the same spectrogram contaminated with 5% additive noise. Here the phase modulator gate  $g(t)$  is driven at 10 GHz with a bandwidth of  $\sim 300$  GHz, similar to the gate bandwidth used in our experiments. This corresponds to  $\sim 15\%$  of the bandwidth of the O-AWG waveform  $a(t)$ , which is assumed to have 200 lines at 10 GHz spacing, with spectral intensities and phases generated randomly. Fig. 6(a) shows a generated spectrogram with  $256 \times 256$  grid, which shows complicated structures. For clarity, only the spectrogram with 5% additive noise is shown. Fig. 6(b) shows example curves of error vs. number of iterations after running the retrieval algorithm. The number of iterations to converge depends on the random initial guesses, which vary with each particular retrieval realization. For the noise-free case, the error is below  $10^{-5}$ , ultimately limited by computer precision. With the 5% noise level, the error is around 0.03 (close to the noise level, as expected). In our simulations, we can successfully retrieve the pulses with as much as 10% additive

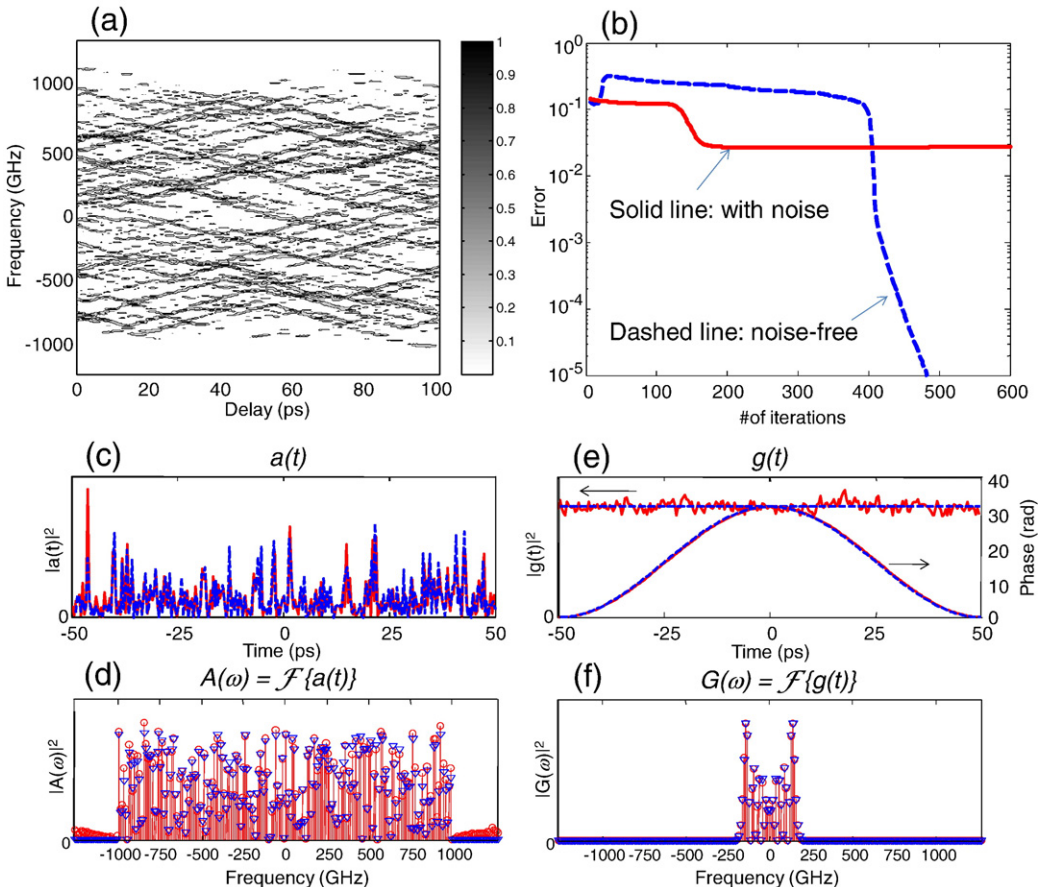


**Fig. 6.** Simulation results for  $a(t)$  with 200 lines. (a) Spectrogram with 5% additive noise. (b) Error vs. # of iterations. Retrieved (c) pulse  $a(t)$ , (d) spectrum  $A(\omega) = \mathcal{F}\{a(t)\}$ , (e) gate  $g(t)$ , and (f) spectrum  $G(\omega) = \mathcal{F}\{g(t)\}$ . Solid line and circles: based on spectrogram with 5% additive noise. Dashed line and triangles: based on noise-free spectrogram. For clarity, only intensities are shown in (c), (d) and (f). Noise-free spectrogram is not shown.

noise. Fig. 6(c) shows the retrieved  $a(t)$  temporal waveform intensity, showing the complexity expected from a 200 line spectrum (retrieved spectrum shown in Fig. 6(d)). The case with noise agrees very well with the noise-free case in both time and frequency domains, showing potential for practical experiments at the 200 line level. Note that in the 5% noise case, the retrieval does return some additional low intensity spectral lines beyond the 200 spectral lines in the input spectrum. Fig. 6(e) shows the retrieved phase modulator gate  $g(t)$ , with a constant temporal intensity and sine temporal phase modulation. For the case of the spectrogram with noise, there is noise on the intensity of the retrieved  $g(t)$ , whereas the strong phase modulation of  $g(t)$  shows essentially no fluctuations even if the spectrogram is noisy. This is consistent with our experimental results as shown in Fig. 2(c). Fig. 6(f) shows the retrieved  $G(\omega)$  showing  $\sim 30$  spectral lines. Again, the noisy case agrees very well with the noise-free case. For clarity, only intensities are shown in (c), (d) and (f).

In our simulation,  $a(t)$  has 200 lines with spectral intensities and phases generated randomly. This results in a waveform with high complexity, with the strong line-by-line phase and amplitude variations that are characteristic of O-AWG. For such high complexity waveforms, generally the retrieval algorithm works very well:  $a(t)$  and  $g(t)$  can be retrieved successfully after very few random initial guesses. Interestingly, if  $a(t)$  remains at 200 lines but is transform limited (spectral phases equal to zeros), many more trials with different initial random guesses must generally be tried before the algorithm will converge. But if  $a(t)$  and  $g(t)$  have comparable bandwidths, usually there are no such issues, even if  $a(t)$  is a transform-limited pulse (as in our experiments shown in Fig. 3).

### 3. Conclusions

In summary, we have demonstrated the applicability of linear spectrogram methods based on electro-optic phase modulation for characterization of high repetition rate optical arbitrary waveforms generated using spectral line-by-line pulse shaping. We demonstrate that this method is applicable even with spectral phase and amplitude changes sufficiently complex that waveforms span the full temporal period for 100% duty cycle. We also show that strongly phase-modulated pulses can be compressed to the bandwidth limit by using a pulse shaper programmed in accord with spectral phase data retrieved using linear spectrograms. The linear spectrogram method provides high spectral resolution, high measurement precision, superior sensitivity, and self-referencing capability, all of which are desirable for O-AWG waveform characterization. Exploration of various approaches, including the method described here, to experimentally characterize O-AWG signals scaled to a substantially larger number of spectral lines and complexity [4] is expected to be the topic of ongoing investigation.

### Acknowledgements

This material is based upon work supported in part by DARPA/ARO under grant W911NF-07-1-0625 (A.M.W.) as part of the DARPA Optical Arbitrary Waveform Generation (O-AWG) program, by the National Science Foundation under grant ECCS-0601692 (A.M.W.), and by the National Institutes of Health, National Cancer Institute, under grant R21 CA115536 (S.A.B.).

The authors thank the Beckman Institute for Advanced Science and Technology, University of Illinois at Urbana-Champaign, for a Beckman Fellowship to Zhi Jiang. They also thank Supradeepa Venkata and Fahmida Ferdous for using their experimental setup.

### References

- [1] A.M. Weiner, Rev. Sci. Instrum. 71 (2000) 1929.
- [2] Z. Jiang, D.S. Seo, D.E. Leaird, A.M. Weiner, Opt. Lett. 30 (2005) 1557.
- [3] S.T. Cundiff, J. Phys. D: Appl. Phys. 35 (2002) R43.
- [4] Z. Jiang, C.B. Huang, D.E. Leaird, A.M. Weiner, Nat. Photonics 1 (2007) 463.
- [5] R.P. Scott, N.K. Fontaine, J. Cao, K. Okamoto, B.H. Kolner, J.P. Heritage, S.J.B. Yoo, Opt. Express 15 (2007) 9977.
- [6] D. Miyamoto, K. Mandai, T. Kurokawa, S. Takeda, T. Shioda, H. Tsuda, IEEE Photon. Technol. Lett. 18 (2006) 721.
- [7] K. Takiguchi, K. Okamoto, T. Kominato, H. Takahashi, T. Shibata, Electron. Lett. 40 (2004) 537.
- [8] R. Trebino, Frequency-Resolved Optical Gating, Kluwer Academic Publishers, 2004.
- [9] C. Iaconis, I.A. Walmsley, Opt. Lett. 23 (1998) 792.
- [10] C. Dorrrer, I. Kang, Opt. Lett. 28 (2003) 1481.
- [11] J.M. Dudley, F. Gutty, S. Pitois, G. Millot, IEEE J. Quantum Electron. 37 (2001) 587.
- [12] Z. Jiang, D.E. Leaird, A.M. Weiner, J. Lightwave Technol. 24 (2006) 2487.
- [13] V.R. Supradeepa, D.E. Leaird, A.M. Weiner, Opt. Express 17 (2009) 25.
- [14] H.X. Miao, D.E. Leaird, C. Langrock, M.M. Fejer, A.M. Weiner, Opt. Express 17 (2009) 3381.
- [15] C. Dorrrer, I. Kang, Opt. Lett. 27 (2002) 1315.
- [16] C. Dorrrer, I. Kang, IEEE Photon. Technol. Lett. 16 (2004) 858.
- [17] C. Dorrrer, I. Kang, J. Opt. Soc. Am. B: Opt. Phys. 25 (2008) A1.
- [18] D. Reid, J. Harvey, IEEE Photon. Technol. Lett. 19 (2007) 535.
- [19] N.K. Fontaine, R.P. Scott, J.P. Heritage, B.H. Kolner, S.J.B. Yoo, Conference on Lasers and Electro-Optics (CLEO 2007), 2007, Paper CFF5.
- [20] K.T. Vu, A. Malinowski, M.A.F. Roelens, M. Ibsen, P. Petropoulos, D.J. Richardson, Conference on Lasers and Electro-Optics (CLEO 2007), 2007, Paper CFF4.
- [21] H. Murata, A. Morimoto, T. Kobayashi, S. Yamamoto, IEEE J. Sel. Top. Quantum Electron. 6 (2000) 1325.
- [22] Z. Jiang, D.E. Leaird, A.M. Weiner, IEEE J. Quantum Electron. 42 (2006) 657.
- [23] J. Bromage, C. Dorrrer, I.A. Begishev, N.G. Usechak, J.D. Zuegel, Opt. Lett. 31 (2006) 3523.
- [24] V.R. Supradeepa, Daniel E. Leaird, Andrew M. Weiner, Opt. Express 17 (2009) 14434.
- [25] N.K. Fontaine, R.P. Scott, J.P. Heritage, S.J.B. Yoo, Opt. Express 17 (2009) 12332.
- [26] D.M. Marom, C. Dorrrer, L. Kang, C.R. Doerr, M. Cappuzzo, et al., The 17th Annual Meeting of the IEEE Lasers & Electro-Optics Society, 2, 2004, p. 585, WP1.
- [27] E.T.J. Nibbering, M.A. Franco, B.S. Prade, G. Grillon, J.P. Chambaret, A. Mysyrowicz, J. Opt. Soc. Am. B: Opt. Phys. 13 (1996) 317.
- [28] J.M. Dudley, L.P. Barry, J.D. Harvey, M.D. Thomson, B.C. Thomsen, P.G. Bolland, R. Leonhardt, IEEE J. Quantum Electron. 35 (1999) 441.
- [29] Y. Mairesse, F. Quéré, Phys. Rev. A 71 (2005) 011401.
- [30] D.J. Kane, IEEE J. Quantum Electron. 35 (1999) 421.